VIII International Conference on Textile Composites and Inflatable Structures
STRUCTURAL MEMBRANES 2017
K.-U.Bletzinger, E. Oñate and B. Kröplin (Eds)

A MULTISCALE NON-ORTHOGONAL MODEL FOR TENSILE PROPERTIES OF UNCOATED AND COATED F-12 ARAMID FABRIC

HUIFENG TAN [*], XILIN LUO, GUOCHANG LIN

[*] Center for Composite Materials and Structures
Harbin Institute of Technology
No.2 Yikuang Street, Harbin, 150080, China
e-mail: tanhf@hit.edu.cn - web page: http://www. hit.edu.cn

Key words: F-12 aramid fabric, multiscale, non-orthogonal, off-axial tensile

Summary. Coated F-12 aramid fabric can be used as the balloon envelopes material because of the high strength and light weight performance. In this paper, a multiscale non-orthogonal material model was established to capture the tensile properties of F-12 fabric with and without polyethylene terephthalate-aluminum (PET-Al) coating. Off-axial monotonic tensile tests were carried out to validate the material model. The nonlinearity and anisotropic properties of the coated and uncoated fabrics were investigated. In this model, the stress was obtained based on the equilibrium equations and yarn constitutive model in mesoscale. The mesoscale configuration was observed through optical microscope and SEM. The material orientation was aligned with the yarn directions and the stress was updated in real time. The material model was implemented by user material subroutine in ABAQUS and simulate fabric off-axial tensile test. In addition, a theory model to calculate the elastic property of the fabric was also set up using the mesoscale deformation mechanism. The simulation results were compared with the test and theory results. Results suggest that simulation results were agree well with test results. The fabrics were nearly linearity in weft direction, while the stress-strain curve exhibited obvious nonlinearity in warp direction. The tensile modulus of the fabric showed orthotropic behaviour rather than the strength. The coating can affect the strength and failure model of F-12 fabric. Yarn slip was the mostly failure model in uncoated fabric while break in coated fabric. Research in this study provides certain reference in analysis and design for balloon envelops.

1 INTRODUCTION

F-12 aramid fibers is spun from aromatic polyamides and copolyamides with heterocycles in the chain, whose strength (4.35-4.67GPa) is 1.69 times higher than that of Kevlar-49. It is developed by the 46th Institute, Sixth Academy of China Aerospace Science & Industry Corp. PET-Al coated F-12 aramid fabric is a suitable envelope material in stratospheric airship and super-pressure balloon. The PET-Al coating contains helium barrier layer and can be utilized to resistant the UV radiation and heat, while the fabric is used as the load carrier layer. The mechanic performance of the envelope membrane is related to the carrying capacity and service life of the aerostatics structures. Hence, the demands for the envelope material are more complex than that of architectural textiles [1].

The coated F-12 aramid fabric is a flexible laminated material, whose mechanic properties are determined by fabric layer. On the early research of fabric mechanics, a basis theoretical

model developed by Pierce [2] was only used to geometrical analysis based on the weave architecture and yarn properties. Kawabata [3], Hearle, et al. [4] detailed and expanded the model to mechanical analysis. The simplifying assumptions made the theoretical model different from the actual fabric. Hence, there are certain limitations in the theoretical analysis results.

In the former research, experiment is another main tool to investigate the mechanical behavior of the fabric [5-6]. Since coated fabric is usually used in tensioned membrane structure and inflatable structure. Hence, tensile test is the most common method, which consist mono-uniaxial test, biaxial test, cyclic test. However, the macroscopic test is unable to capture the deformation mechanism in yarn scale. The mesoscale or multiscale numerical analysis approach combined with experimental method was commonly carried out to study the systematic information of the tensile behavior of fabric.

Due to the hierarchical of the fabric, numerical method [7] can be divided into three categories, including microscopic (fiber level), mesoscopic (the yarn level) and macroscopic (the fabric level). The homogenization method, which takes the yarns and fabric as a continuum, is required in mesoscopic and macroscopic approach. Usually, the solid element and shell element are used to simulate the yarn and fabric. Many deformation and the inter-fiber or intra-fiber interaction mechanisms are ignored. The result is that as the scale increase, the computational efficiency improved, while the accuracy reduced. Some researchers developed the multiscale material model, which is a macroscale models based on mesoscale properties. However, most of their study focused on dry fabric. In this paper, a multiscale material model based on mesoscale behavior was developed to simulate the coated and uncoated fabric. The coating properties and yarn bending and shear responses were considered. The off-axial tensile tests were carried out to verify the material model. The extension responses, such as the anisotropic properties, tensile strength, deformation field, elongation at break and failure modes were analyzed. The effect of the PET-Al coating to the aramid fabric was investigated.

2 EXPERIMENTAL PROGRAMS

2.1 Test material and specimens

In this study, a plain weave fabric made of F-12 aramid fibers with and without PET-Al coating were investigated, as shown in Fig. 1. The line density of the yarn is 23 tex and the weave density is 16 yarns/cm. The uncoated fabric shows 60.2g/m^2 area density with a thickness of 0.130mm. The coated fabric shows 127g/m^2 area density with a thickness of 0.177mm. The surface morphology and cross section shape of the fabric are investigated by SEM and optical microscope respectively, as shown in Fig. 2. The figures were imported into AutoCAD software and then the structural parameters were calibrated, as shown in Tab. 1.

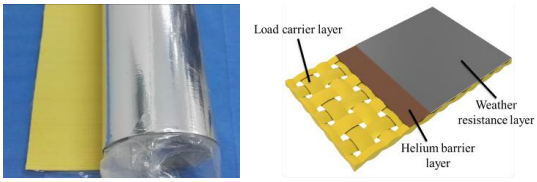

Fig. 1 F-12 aramid fabric with PET-Al coating

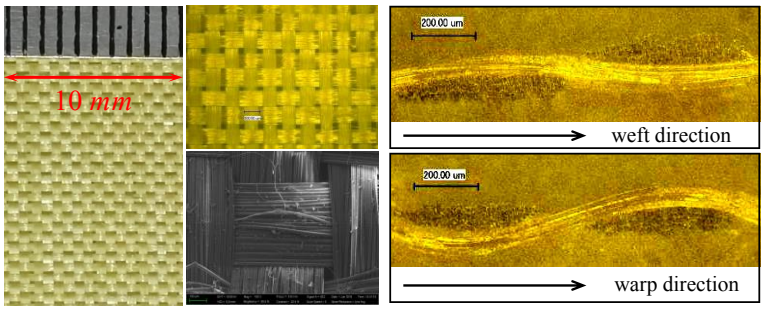

Fig. 1 Macro and mesostructure of F-12 fabric: surface morphology (left) ;cross section (right)

Tab. **1** Material properties and unit cell geometry for F-12 fabric

Properties	Values
Yarn count (yarn/cm) warp/weft	16
Yarn linear density (tex) warp/weft	23
Fiber density (g/cm3)	1.44
Yarn spacing (mm) warp/weft	0.584 / 0.672
Yarn width (mm) warp/weft	0.523 / 0.470
Yarn height (mm) warp/weft	0.068 / 0.074
Crimp amplitude (mm) warp/weft	0.072 / 0.015
Crimp length (mm) warp/weft	0.703 / 0.586
Yarn inclined angle (°) warp/weft	16 / 3
Crimp (%) warp/weft	4.61 / 0.34
Fabric thikness (mm)	0.13

Mono-uniaxial extension tests with seven different off-axis angles (θ=0°, 15°, 30°, 45°, 60°,75°, 90°) were conducted , according to the standard of ISO 1421-1998. The samples for the coated and uncoated fabrics were tailored into long strips by 300 × 50 mm, with four aluminum reinforced plates pasted on the end of the samples. The angle between the warp direction and the loading direction was defined as off-axis angle, as shown in Fig. 3. In coordinate system *OXY*, *X*-axle and *Y*-axle indicate the warp and weft direction, respectively, while in *Oxy*, axis *x* represents loading direction. The tests were conducted using INSTRON 5965 at the loading rate of 50mm/min. Both video extensometer and digital image correlation (DIC) were used to measure the strains, as shown in Fig. 4.

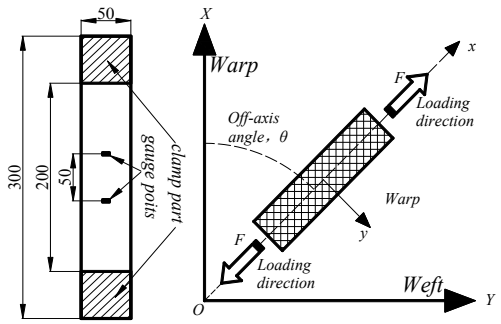

Fig. 2 Geometry and the tailor direction of the off-axes extension sample

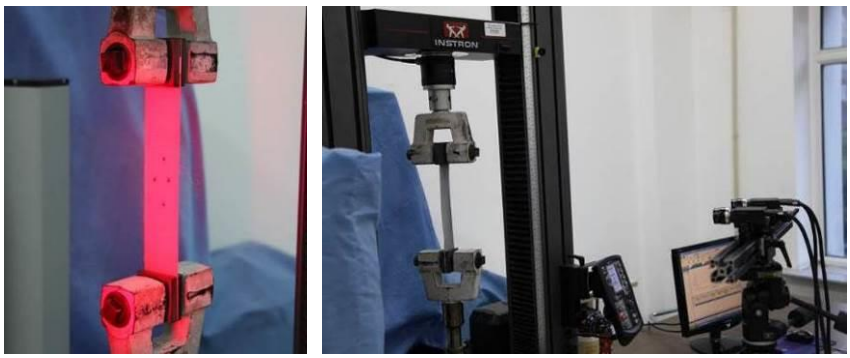

Fig. 3 Deformation measurement in tensile test (a)video extensometer (b)DIC

The yarn tensile properties are required in the multiscale model. Hence，yarn extension test was carried out refer to ASTM D2256. The sample was extract from fabric exactly. The yarn sample was cut into 350mm. Aluminum plates with the size 30mm × 50mm were pasted at the end of the sample. The effective cross section area can be calculated by the linear density and the volume density.

All the tests are conducted in the tensile test machine INSTRON5965. Two different load cells with loading range in 0-0.5KN and 0-5KN are used in yarn test and fabric test, respectively.

3 NUMERICAL SIMULATED

3.1 Material model based on meso-structure

The mechanical behavior is related to the fiber properties and yarn woven architecture. As seen in Fig. 2, F-12 fabric shows a repetitive orthogonal configuration that warp yarns interlace weft yarns one by one. It means that a representative element can be built to analyze the entire structure. In this study, a shell element which contains the cross-over point and yarns with half lengths of unit cell based on meso-structure was established, to relate macroscale material model to yarn scale, as shown in Fig. 5. The shell element is orthotropic at the initial state. In the case of shear deformation, the warp yarns and the weft yarns would rotate around the cross-over points. The angle between warp and weft yarns changed with the deformation. Hence, the shell element will be non-orthotropic. An actual material model requires the material orientation in the shell element tracking with the yarns direction in real time [8-9]. The coating will shear the load. Especially in the shear case, coating would increase the shear resistance obviously. In the case of coated fabric, coating stretching and shear items were added to the uncoated fabric model.

3.2 Tracking yarn direction

Off-axes extension test would cause shear deformation. As mentioned before, the fiber orientation has been constantly changing in the test. Based on the theory of continuum mechanics, the fiber orientation can be tracked as the following method.

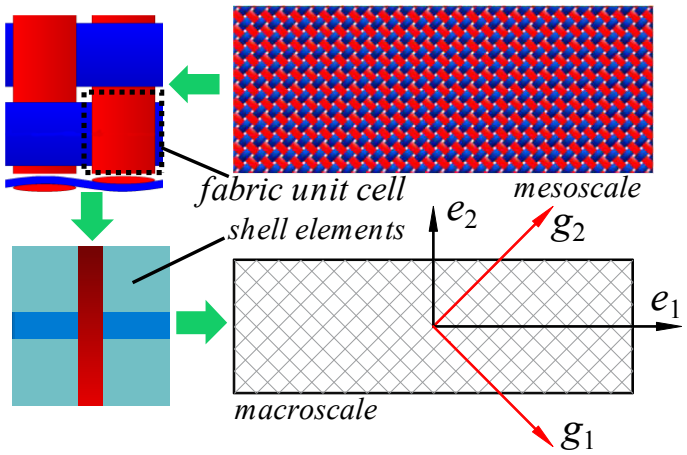

Fig. 5 The principle of non-orthogonality macro-model based on mesoscale

The coordinate systems on the fabric before and after deformation are shown in Fig. 6. $\boldsymbol{e_i}$ was the orthogonal local frame attached to the element which is called co-rotational frame. $\boldsymbol{g_i}$ was a non-orthogonal frame attached to the yarn directions. The new yarn orientation can be calculated from the initial vectors and the deformation gradient, while the new co-rotational frame can be related to the initial vectors and the rotational gradient, as shown in formula (1) and (2):

$$\boldsymbol{g}_i = \boldsymbol{F} \cdot \boldsymbol{g}_i^0 \tag{1}$$

$$\boldsymbol{e}_i = \boldsymbol{R} \cdot \boldsymbol{e}_i^0 \tag{2}$$

$$\boldsymbol{R} = \boldsymbol{F}\boldsymbol{U}^{-1} \tag{3}$$

where $\boldsymbol{F}$ represents the deformation gradient, $\boldsymbol{U}$ is the right-stretch tensor, $\boldsymbol{R}$ is the rotational tensor. $\boldsymbol{g}_i^0$ and $\boldsymbol{e}_i^0$ are the initial unit vectors of material frame and co-rotational frame, respectively.

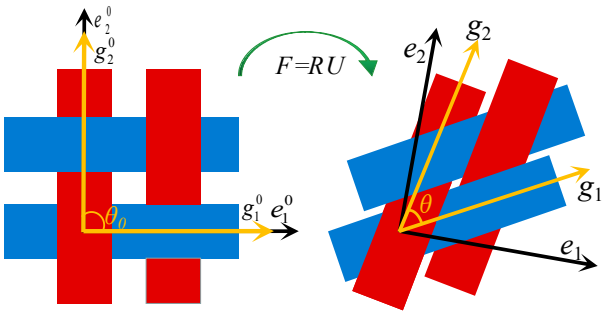

Fig. 6 The coordinate systems on the fabric (a)before deformation (b)after deformation

The current yarn stretch can be determined from:

$$\lambda_i = \sqrt{\boldsymbol{g}_i^T \cdot \boldsymbol{g}_i} = \sqrt{(\boldsymbol{F} \cdot \boldsymbol{g}_i^0)^T \cdot (\boldsymbol{F} \cdot \boldsymbol{g}_i^0)} = \sqrt{\boldsymbol{g}_i^{0T} \cdot \boldsymbol{C} \cdot \boldsymbol{g}_i^0}\ , \quad \boldsymbol{C}=\boldsymbol{F}^T\boldsymbol{F} \tag{4}$$

where ***C*** is the Green deformation tensor. The angle between the warp yarns and weft yarns can be calculated by the following formulas:

$$\cos\theta = \frac{g_1^{0T} C g_2^0}{\lambda_1 \lambda_2} \tag{5}$$

Hence, the shear angle is defined as following:

$$\gamma = \frac{\pi}{2} - \theta \tag{6}$$

3.3 Determination of stress

After shear deformation, the balanced force generated on the boundary of the shell element is shown in Fig. 7. The relationship between each force components can be established through the equilibrium equation [9].

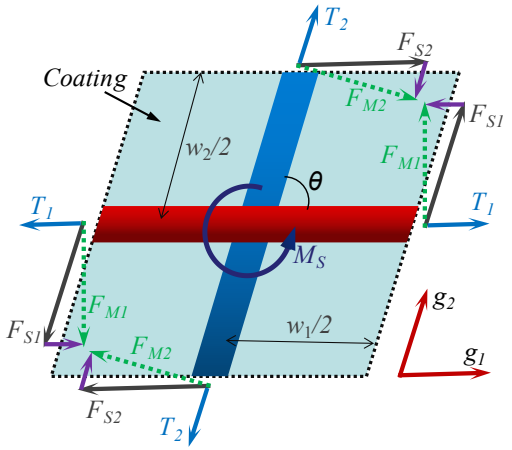

Fig. 7 Forces balance at the boundaries of unit cell

The shear force on the boudary can be determined by following formulas:

$$F_{Mi} = \frac{M_S}{w_i}; i = 1,2 \tag{7}$$

$$F_{Si} = {}^{F_{Mi}}\!/_{\sin\theta}; i = 1,2 \tag{8}$$

The traction force vector is defined as:

$$\boldsymbol{t} = \boldsymbol{\sigma} \boldsymbol{n} dS \tag{9}$$

Where ***t***, ***σ***, ***n***, ***dS*** are the traction force vector, Cauchy stress tensor, the unit normal of the surface, and small surface area. In conclusion, the Cauchy stress can be decided by yarn tension $f_{yarn,1}$, coating tension $f_{ct,1}$, yarn bending moments M_{bi}, the shear force F_{Si}:

$$\sigma_{11} = \frac{f_{yarn,1} \cdot \cos\theta_1 + f_{ct,1} - M_{b1} / (l_1 \cdot \sin\theta_1) - F_{S1} \cdot \cos\theta}{A_2 \sin\theta}; \tag{10}$$

$$\sigma_{22} = \frac{f_{yarn,2} \cdot \cos\theta_2 + f_{ct,2} - M_{b2} / (l_2 \cdot \sin\theta_2) - F_{S2} \cdot \cos\theta}{A_2 \sin\theta}; \tag{11}$$

$$\sigma_{12} = \sigma_{21} = \frac{F_{S1}}{A_2} = \frac{F_{S2}}{A_1} = \frac{F_S}{w_1 w_2 t_f^0 \sin^2\theta} \tag{12}$$

3.4 Constitutive relations

As indicated above, the material model estabished was based on the yarn mechanical properties and geometry. From formula (10), the yarn tensile and bending constitutive relation, the coating tensile behavior, the fabric shear behavior are requiered.

The tansile force in the yarns is determined by:

$$f_{yarn,i} = E_i(\varepsilon_i) A_i \varepsilon_i \tag{13}$$

The tansile force in the coaing is determined by:

$$f_{ct} = E_{ct} A_{ct} \varepsilon_i \tag{14}$$

The bending behavior of the yarns are calculated from:

$$M_{bi} = k_{bi}\left(\theta_i - \theta_i^0\right) \tag{15}$$

The fabric shear behavior is determined by bias tensile test. Polynomial function is used to fit the relation between normalized shear force and shear angle. Then, the parameters are obtanied.

$$F_{sh}(\gamma) = \frac{1}{(2D - W)\cos(\gamma)}\left(\frac{FD}{W}(\cos(\frac{\gamma}{2}) - \sin(\frac{\gamma}{2})) - W\cos(\frac{\gamma}{2})F_{sh}\left(\frac{\gamma}{2}\right)\right) \tag{16}$$

$$F_{sh}(\gamma) = a\gamma^5 + b\gamma^4 + c\gamma^3 + d\gamma^2 + e\gamma + f \tag{17}$$

4 THEORETICAL MODEL

According to mesosopic model, the elastic constant of the fabric can be calculated based on energy method and Castigliano's theorem [10]. three dimensional sawtooth model was established to model the unit cell of fabric, as shown in Fig. 7. At initial state or on-axial tensile deformation, the warp yarns and weft yarns are orthogonal. The tensile mechanism are crimp change and yarn extension. The main load on the yarns are tensile force and bending moment. In Fig. 8, f_i is the in-plane axial tensile loading, which is decomposed into the yarn part (f_{yarn}) and the coating part (f_{ct}). v_i is the compress loading between warp yarns and weft yarns.

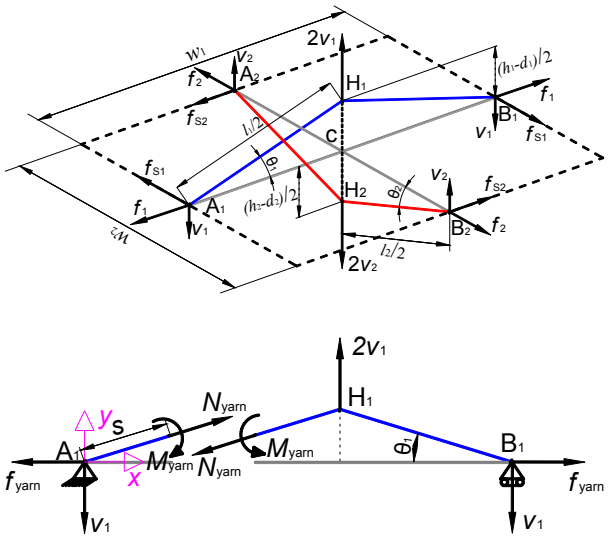

Fig. 8 The force analysis of the saw-tooth model

The extension strain energy of the yarn is given as:

$$U_{yarn,E}=\frac{l_1\left(f_{yarn,1}\cos\theta_1+v_1\sin\theta_1\right)^2}{2E_1A_1}+\frac{l_2\left(f_{yarn,2}\cos\theta_2+v_2\sin\theta_2\right)^2}{2E_2A_2} \tag{18}$$

The bending strain energy of the yarn is given as:

$$U_{yarn,B}=\frac{{l_1}^3\left(-f_{yarn,1}\sin\theta_1+v_1\cos\theta_1\right)^2}{24E_1I_1}+\frac{{l_2}^3\left(-f_{yarn,2}\sin\theta_2+v_2\cos\theta_2\right)^2}{24E_2I_2} \tag{19}$$

The total strain energy of the yarn is given as:

$$U_T=U_{yarn,E}+U_{yarn,B} \tag{20}$$

The elastic modulus in uniaxial loading can be determined as:

$$E_1=\frac{12B_1w_2}{w_1{l_1}^3\sin^2\theta_1}\left(1+\frac{B_2{l_1}^3\cos^2\theta_1}{B_1{l_2}^3\cos^2\theta_2}\right) \tag{21}$$

where l_i is the yarn length, w_i is the yarn spacing, h_i is the crimp amplitude, θ_i is theyarn incline angle, B_i is the yarn bending stiffness, which can be calculated from $B=EI$. Then, the bending stiffnesses are obtained, B_{warp}=0.56 N.mm^2, B_{weft}=0.63N.mm^2. Plug the values in Tab. 1 and the bending stiffness into formula (23), the theoretical value of initial modulus can be calculated.

5 RESULTS AND DISSCUSSION

5.1 Test results

The yarn tensile behavior is shown in Fig. 9. Solid lines and dashed lines represent warp direction and weft direction, respectively. Five effective samples were test in each type of yarns. The stress-strain curves of each type of yarns show excellent repetition, which indicate the performance and the fiber damge in weaving process are stable. The piecewise linear functions are used to fit the curves. Then, the tensile modulus are obtained:

$$E_{weft}=\begin{cases}119.04\ \ GPa;\ \ \varepsilon\le 0.01\\ 83.24\ \ GPa;\ \ \varepsilon>0.01\end{cases}\text{, in weft direction}$$

$$E_{warp}=\begin{cases}64.65\ \ GPa;\ \ \varepsilon\le 0.25\%\\ 112.41\ \ GPa;\ \ 0.25\%<\varepsilon\le 1\%\\ 79.75\ \ GPa;\ \ 1\%\le\varepsilon\end{cases}\text{, in warp direction}$$

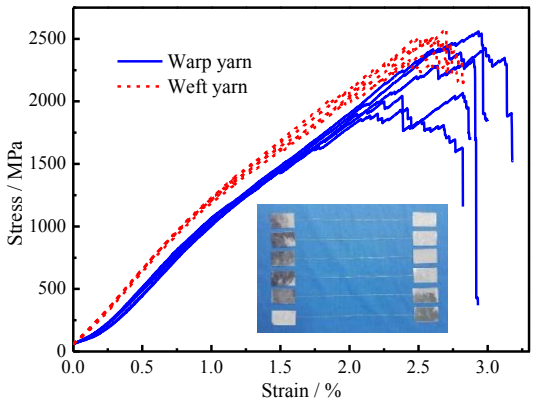

Fig. 9 The stress-strain relation of F-12 single yarn

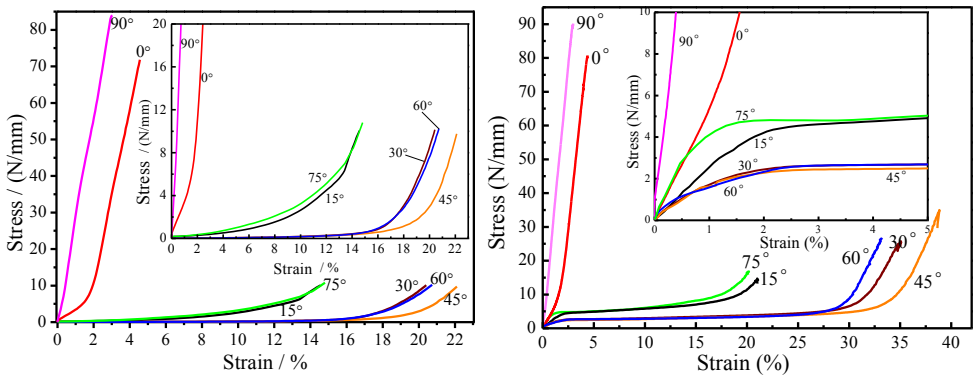

Fig. 10 The stress-strain curves of membrane material (a)uncoated fabric (b)coated fabric

The on-axial and off-axial extension performance is seen in Fig. 10. The modulus of on-axial samples is greater than that of off-axial samples both for uncoated and coated fabric. The relation on the weft direction is linear, while nonlinear in warp direction. It can be explained from Fig.2, the crimp in warp yarns is significantly larger than that in weft yarns. For the complementary angles 15 ° and 75 ° or 30 ° and 60 °, the curves are approximated, which means the fabric is orthogonal. The elongation is increase with the bias angles and

come to maximum value at 45 °. Then the elongation decrease with the bias angles increase. The difference between the uncoated and coated fabric is that the resistance in the cross-over points of coated fabric is greater than that of uncoated fabric. It caused that in the initial bias tensile curves, the loading between the interwoven yarns need to come to the limit static friction to rotate. Hence, the tangent modulus of coated fabric is larger than that of uncoated fabric.

The tensile strength and the failure modes of uncoated and coated fabric are shown in Fig.11 and Fig. 12, respectively. Both for uncoated and coated fabric, the values of breaking forces of on-axial samples are larger than that in other directions. For the uncoated fabric, the values of breaking forces of the samples are decrease with the bias angles and come to minimum values at 45 °. Then the breaking force increase with the bias angles increase. The trend is similar to classical laminate theory. However, the breaking force for the complementary angles of 30 ° and 60 ° are larger than for angles of 15 ° and 75 °. The breaking force for an angle of 45 ° increases as compared to other different bias angles. This probably due to the resistance pf PET-Al coating to the yarn rotation makes the force increases when the direction of the force are coinciding the direction of yarns. Another effect of the coating to the fabric is the failure modes. The failure mode of on-axial uncoated samples is fiber fracture, while interface damage appears in coated samples. For off-axial uncoated samples, the necking effect due to yarn slips occurs, while for coated samples, the samples breaking because of shear failure in intra-yarns.

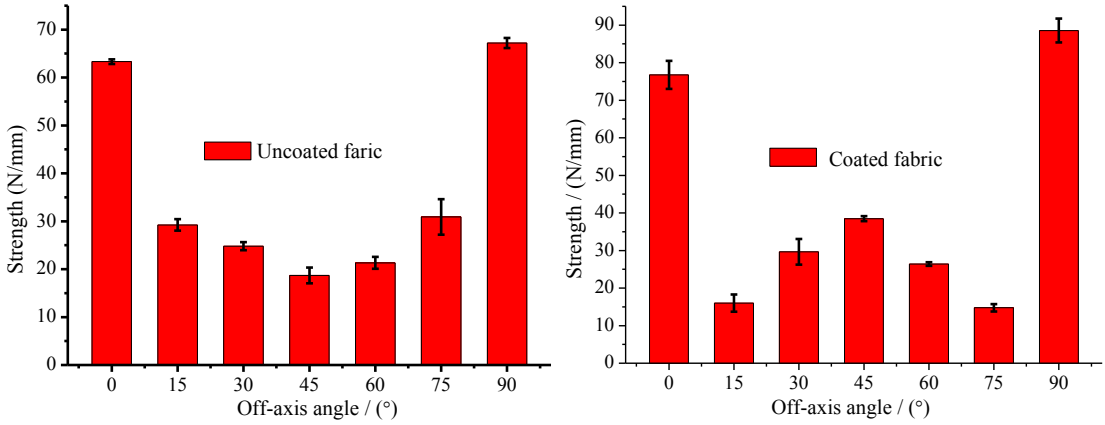

Fig. 11 The tensile strength of membrane material

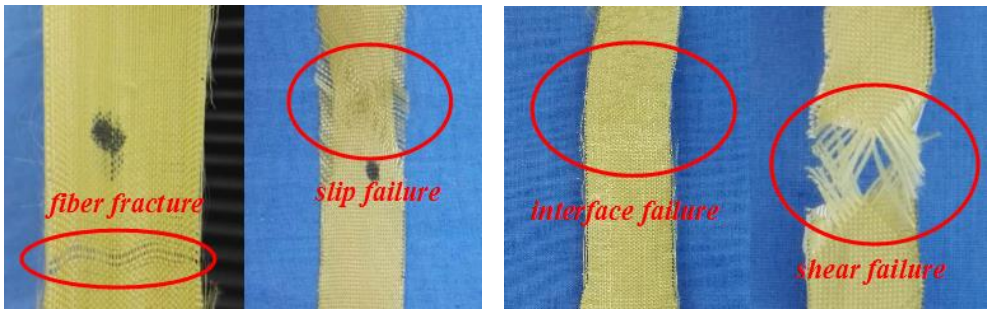

Fig. 12 Damage modes of membrane material: uncoated fabric (left), coated fabric (right)

5.2 Numerical simulation results

Fig. 13 shows the load-extension relation for 45° off-axial tensile of uncoated and coated fabric. The discrete points represent test results, while the lines are FEM results. Blue represent the results of uncoated fabric and red represent that of coated fabric. FEM results agree well with the experiment results. The PET-Al coating affects the shear properties of the fabric obviously. The value elongation of coated fabric is larger than that of uncoated fabric. Besides, at the initial state, the shear stiffness of coated fabric is greater than that of uncoated fabric. This is due to the resistance of the coating to the yarns rotation.

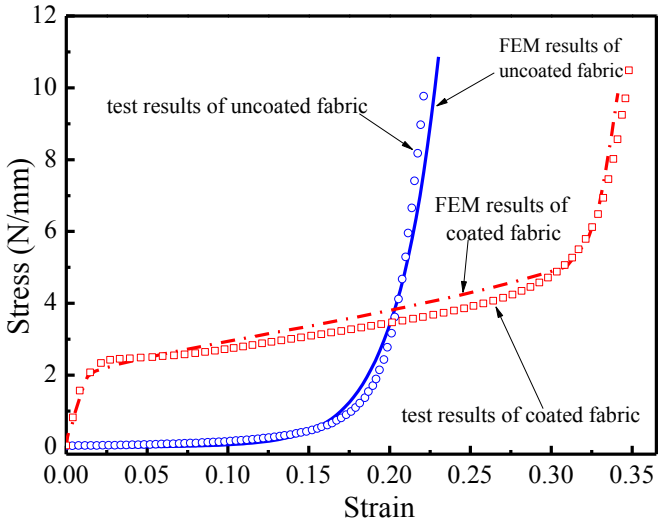

Fig. 13 Load-extension relation for 45° off-axial tensile of uncoated and coated fabric

Fig. 14 and Fig. 15 are the compared deformation results of FEM and experiment for the uncoated and coated fabric on off-axial tensile, respectively. Left side of Fig. 14 is the shear angle contour obtained by FEM. The other side is the actual deformation in tensile test. The deformation is basically symmetrical. However, out-plane displacement appears in the experiment, which is not consider in this material model. Fig. 15 shows the displacement contours obtained by FEM (left) and DIC (right). Both the distribution and the values are agreement. Therefore, the accuracy of the model is further validated.

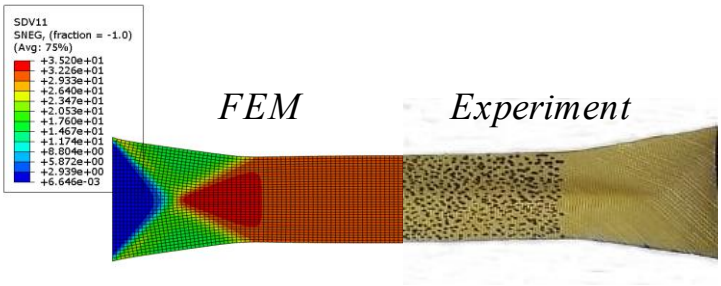

Fig. 14 The FEM results compared with test results on 45° off-axial tensile of uncoated fabric

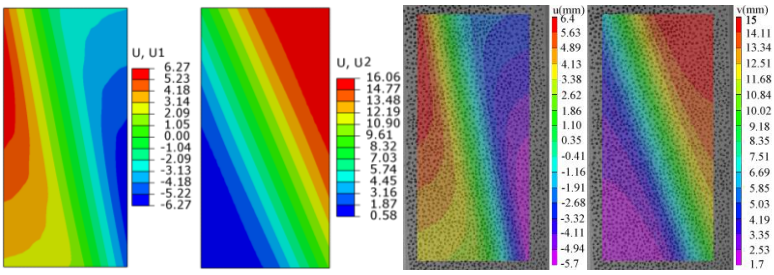

Fig. 15 The FEM results compared with test results on 15° off-axial tensile of coated fabric

6 CONCLUSIONS

In this paper, a multiscale non-orthogonal material model based on mesoscopic properties was established to capture the tensile properties of F-12 fabric with and without PET-Al coating. Off-axial tensile tests were conducted to validate the model and investigate the tensile properties. 15° and 45° test results were taken to compare with the simulation results. The simulation results by the material model agreed well with the experiment of the fabric. The test results show that both uncoated fabric and coated fabric are orthogonal. The PET-Al coating will affect the tensile properties and failure modes of the fabric.

REFERENCES

[1] F. Wang, Y. Chen, W. Xu, et al. “Experimental study on uniaxial tensile and welding performance of a new coated fabric for airship envelopes”, *J. Text. Inst.*, 46(7): pp. 1474-1497, (2017).

[2] F. T. Peirce, "The geometry of cloth structure." *J. Text. Inst.* , 28.3: T45-T96, (1937).

[3] S. Kawabata, M. Niwa and H. Kawai, “The finite deformation theory of plain-weave fabrics. part III-the shear-deformation theory”, *J. Text. Inst.*, vol. 64(2), pp. 62–85, (1973).

[4] Hearle, J. W. S., and W. J. Shanahan. "11—An energy method for calculations in fabric mechanics part i: principles of the method." *J. Text. Inst.*, 69.4, pp. 81-91, (1978).

[5] Y.Y. Zhang, J.H. Xu, and Q.L. Zhang. "Advances in mechanical properties of coated fabrics in civil engineering", *J. Ind. Text.*, 1528083716679159, (2016).

[6] J.H. Hu, C.J. Gao, S.Z. He, et al. "Effects of on-axis and off-axis tension on uniaxial mechanical properties of plain woven fabrics for inflated structures", *Compo. Struc.*, Vol. 171, pp. 92-99, (2017).

[7] M. V. d’Agostino, , Giorgio, I., et al. "Continuum and discrete models for structures including (quasi-) inextensible elasticae with a view to the design and modeling of composite reinforcements", *Int. J. Solids. Struct.*, 59, 1-17. (2015)

[8] O. Erol, B. Powers and M. Keefe, "Development of a non-orthogonal macroscale material model for advanced woven fabrics based on mesoscale structure", *Compos. Part B-Eng.*, Vol. 110, pp. 497-510, (2017).

[9] M. J. King, P. Jearanaisilawong and S. Socrate. "A continuum constitutive model for the mechanical behavior of woven fabrics", *Int. J. Solids Struct.*, Vol. 42.13, pp. 3867-3896, (2005).

[10] Leaf, G. A. V., and K. H. Kandil. "1—The initial load–extension behaviour of plain-woven fabrics." *J. Text. Inst.*, 71.1, pp. 1-7, (1980).